Electronic Supplementary Information for

Enhanced plasmonic sensing of single gold nanoparticles with narrowed resonance linewidths

Shuangshuang Wang,[a] Huatian Hu,[b] Xiaoze Liu*[a] and Tao Ding*[a]

[a]Key Laboratory of Artificial Micro- and Nano-structures of Ministry of Education of China, School of Physics and Technology, Wuhan University, Wuhan 430072, China. E-mails: t.ding@whu.edu.cn (T. Ding); xiaozeliu@whu.edu.cn (X. Liu)

[b]Hubei Key Laboratory of Optical Information and Pattern Recognition, Wuhan Institute of Technology, Wuhan 430205, China.

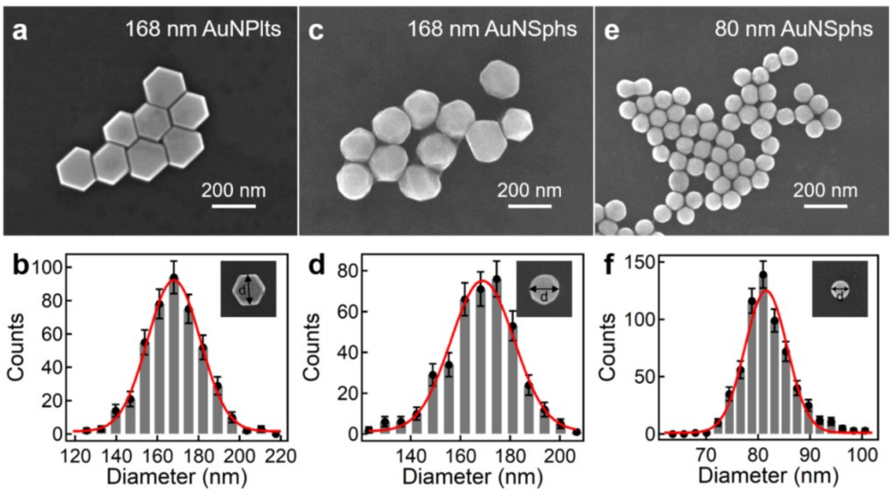

Fig. S1. Characterizations of the Au NPs used in this paper. SEM images of (a) Au NPlts, (c) Big Au NSphs, (e) Small Au NSphs and corresponding diameter distributions of (b) Au NPlts (168±16 nm), (d) Big Au NSphs (168±14 nm), (c) Small Au NSphs (81±6 nm).

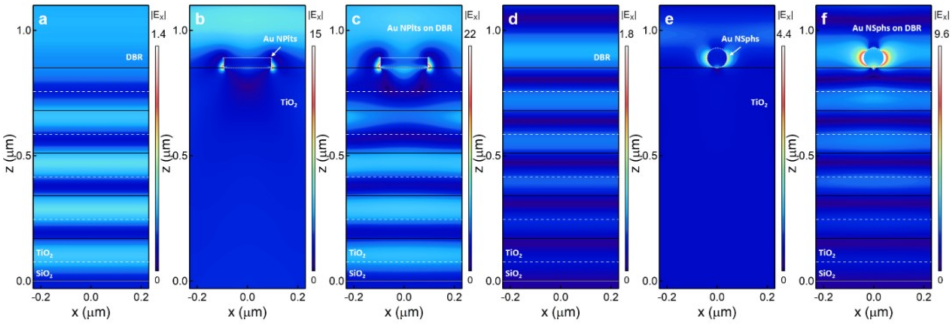

Fig. S2. Near field simulations. The simulatedE-field distributions of (a) DBR substrate only, Au NPlt on (b) TiO_2 substrate, and (c) on DBR substrate. The dashed lines represent the layer interfaces of DBRs and Au NPlts. Excitation wavelength: 728 nm. (d) DBR, Au NSphs on (e) TiO_2, and (f) Au NSphs on DBRs. The dashed lines represent the layer interfaces of DBRs and Au NSphs. Excitation wavelength: 530 nm.

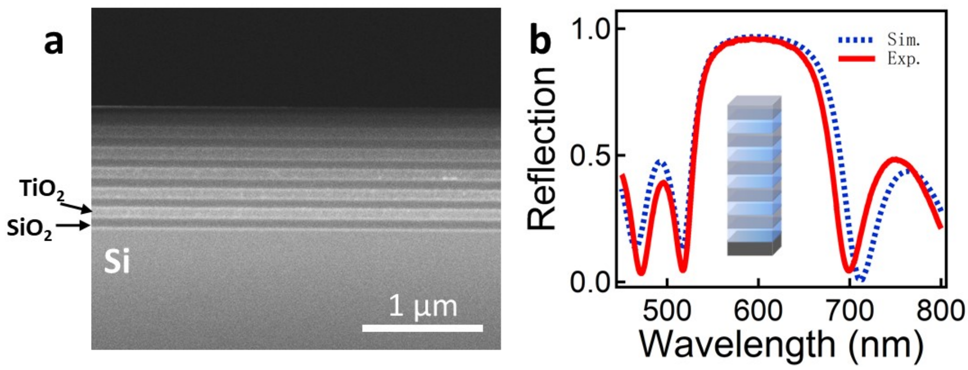

Fig. S3. Characterization of DBR. (a) SEM image of DBR cross section and (b) corresponding reflection spectrum at normal incidence angle (Red solid line). Dashed line represents the simulated reflection spectrum which agrees quite well with experiments.

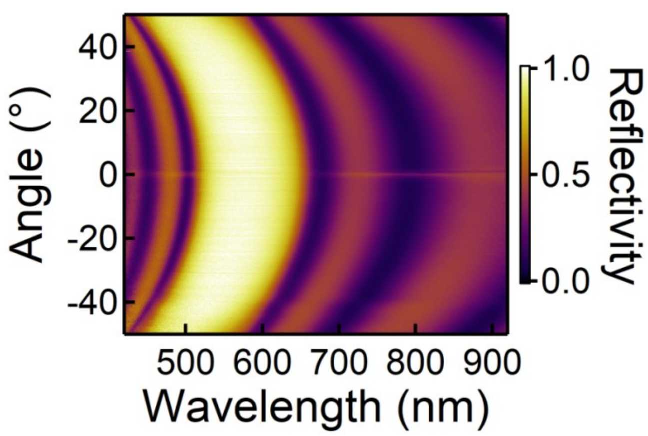

Fig. S4. Angle resolved reflectivity spectroscopy of DBR samples.

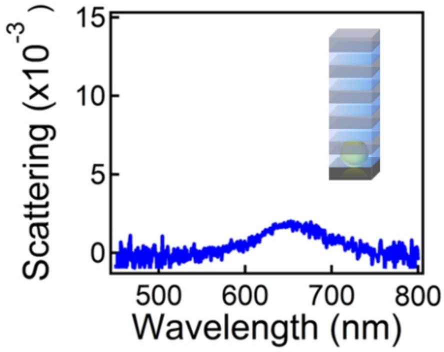

Fig. S5. Dark field scattering spectrum of Au NSphs (80 nm) underneath the DBR. The split peaks disappear with one broad scattering peak.

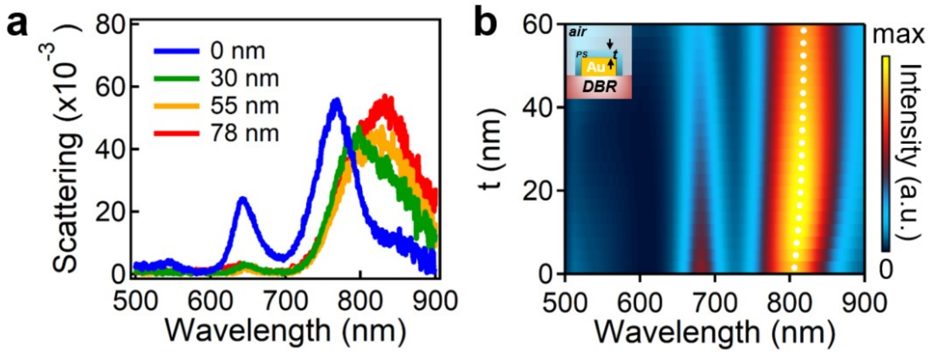

Fig. S6. Influence of the dielectric coating on the scattering spectra of Au NPlts-DBR hybrid structures. (a) Scattering spectra of Au NPlts on DBR coated with PS layer of different thicknesses. (b) Simulated dark field scattering spectra of Au NPlts on DBR with different thickness of PS coatings.

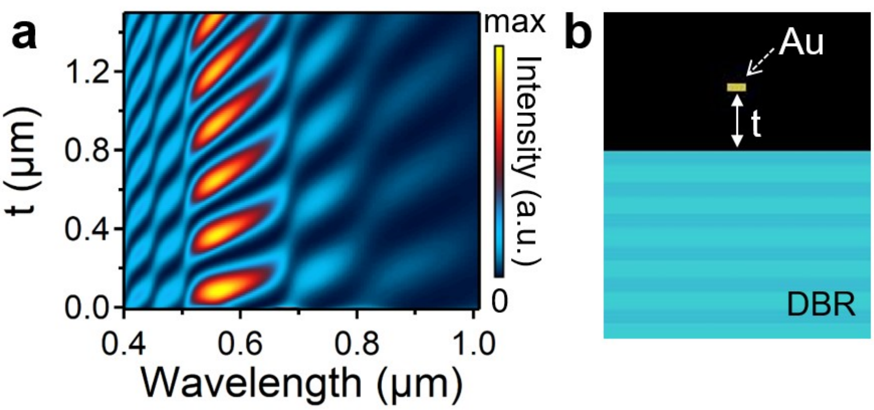

Fig. S7. Simulations of Au NPlts on top of DBR with different spacing. (a) Change of scattering spectra with separation between Au NPlts and the DBR. (b) Schematic of the simulated structure. The t denotes the distance between Au NPlts and DBR surface.

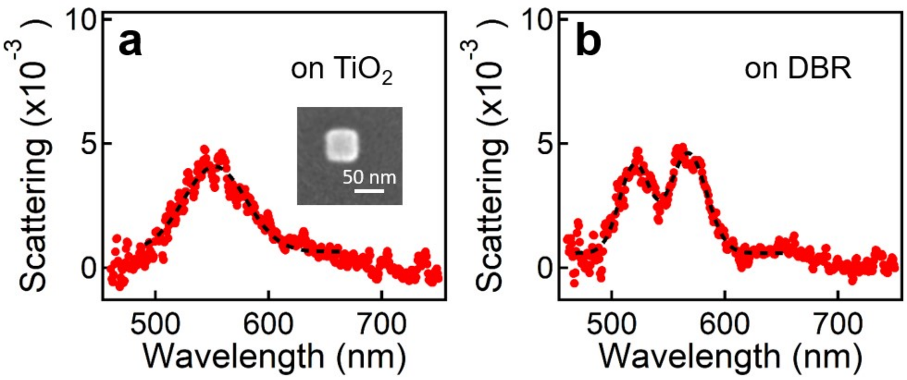

Fig. S8. Narrowed plasmonic peaks of Au NCbs-DBR hybrid structures. Scattering spectra of 50 nm Au NCbs on (a) TiO2/Si (inset is the SEM image of the Au NCbs) and (b) DBR substrate.

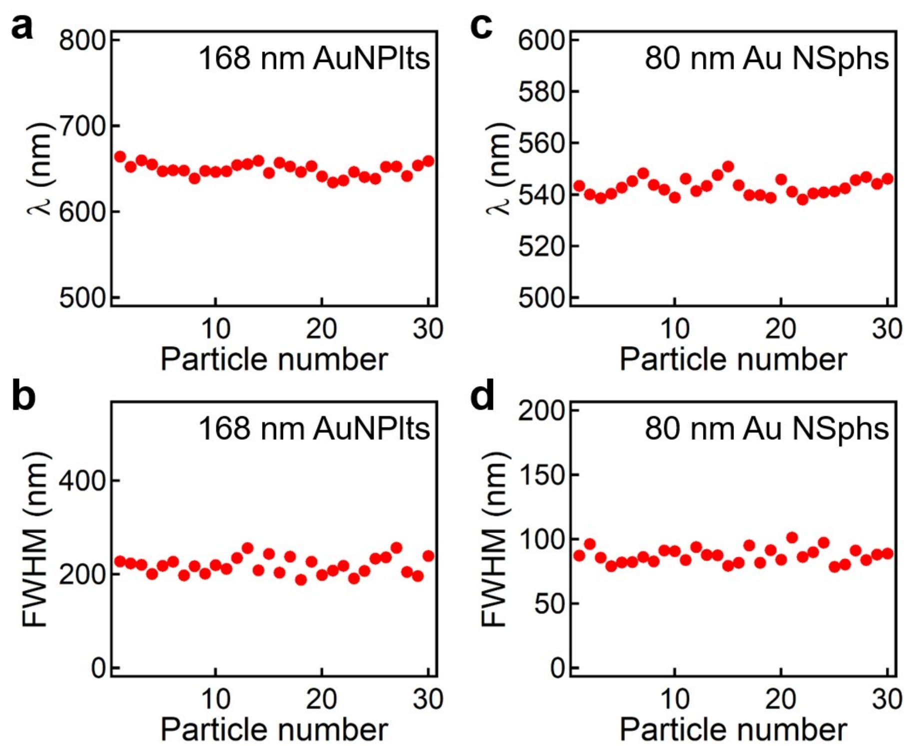

Fig. S9. Statistics of plasmonic resonances and FWHMs of different NPs. (a) Plasmonic resonances and (b) FWHM of Au NPlts on TiO_2 substrate, where $\lambda = 649 \pm 8\, nm, FWHM = 218 \pm 18\, nm$. (c) Plasmonic resonances and (d) FWHM of Au NSphs on TiO_2 substrate, where $\lambda = 543 \pm 4\, nm, FWHM = 87 \pm 6\, nm$.

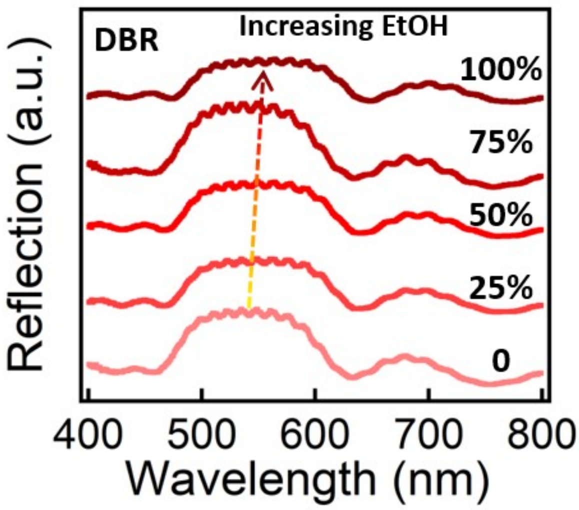

Fig. S10. Sensing measurement based on DBR. Change of reflection spectra of DBR with increasing amount of EtOH.

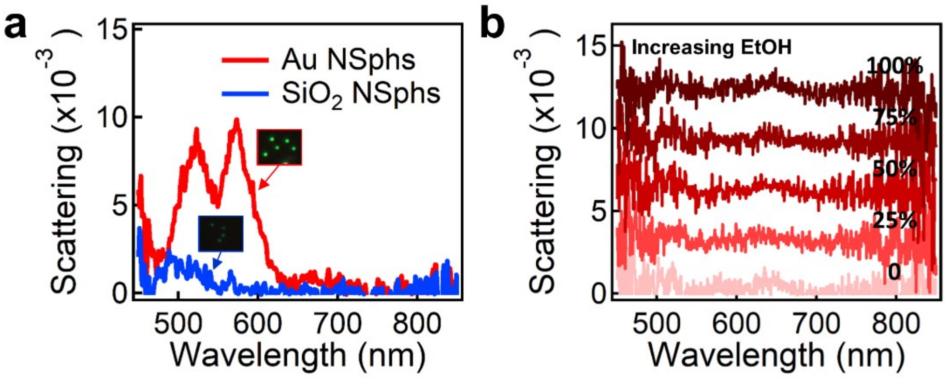

Fig. S11. Scattering spectra and sensing performance of SiO_2 NSphs-DBR hybrid structures. (a) Scattering spectra of Au NSps (80 nm) and SiO_2 NSphs (80 nm) on DBR. Insets are their DF image. (b) Scattering spectra of SiO_2 NSphs (240 nm) on DBR with increasing amount of EtOH.